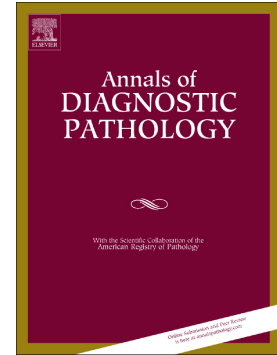


Journal Pre-proof

High-grade sinonasal carcinomas and surveillance of differential expression in immune related transcriptome

Diana Bell, Achim Bell, Renata Ferrarotto, Bonnie Glisson, Yoko Takahashi, Gregory Fuller, Randal Weber, Ehab Hanna



PII: S1092-9134(20)30168-4

DOI: <https://doi.org/10.1016/j.anndiagpath.2020.151622>

Reference: YADPA 151622

To appear in:

Please cite this article as: D. Bell, A. Bell, R. Ferrarotto, et al., High-grade sinonasal carcinomas and surveillance of differential expression in immune related transcriptome, (2018), <https://doi.org/10.1016/j.anndiagpath.2020.151622>

This is a PDF file of an article that has undergone enhancements after acceptance, such as the addition of a cover page and metadata, and formatting for readability, but it is not yet the definitive version of record. This version will undergo additional copyediting, typesetting and review before it is published in its final form, but we are providing this version to give early visibility of the article. Please note that, during the production process, errors may be discovered which could affect the content, and all legal disclaimers that apply to the journal pertain.

© 2018 Published by Elsevier.

High-grade sinonasal carcinomas and surveillance of differential expression in immune related transcriptome

Diana Bell, MD,^{1, 2} Achim Bell, PhD,¹ Renata Ferrarotto, MD,³ Bonnie Glisson, MD,³ Yoko Takahashi, PhD,² Gregory Fuller, MD, PhD,¹ Randal Weber, MD,² Ehab Hanna, MD²

¹Departments of ¹Pathology, ²Head and Neck Surgery, ³Thoracic-Head and Neck Medical Oncology, The University of Texas MD Anderson Cancer Center, 1515 Holcombe Blvd. Houston, TX 77030

Running title: High-grade sinonasal carcinomas

Corresponding author:

Diana Bell

University of Texas MD Anderson Cancer Center, 1515 Holcombe Blvd., Houston, TX 77030

Phone: 713 792-2041; Fax: 713 745-0778

diana.bell@mdanderson.org

Key words: sinonasal, high-grade carcinoma, immune, transcriptome, PRAME

Key words: sinonasal, high-grade carcinoma, immune, transcriptome, PRAME.

Abstract

The skull base is the location of a wide variety of malignant tumors. Among them is sinonasal undifferentiated carcinoma (SNUC), a highly aggressive sinonasal neoplasm that was recently

reclassified into subgroups of high-grade carcinomas with unique genomic events (e.g., SMARC-deficient carcinoma, nuclear protein in testis NUT carcinoma). Other high-grade carcinomas in this location are neuroendocrine carcinomas, sinonasal adenocarcinomas, and teratocarcinosarcomas. Given the rarity of these tumors, little transcriptomic data is available. The aim of this study was to characterize the immunology gene expression profile in SNUC and other high-grade sinonasal carcinomas.

Next-generation sequencing was performed in 30 high-grade sinonasal carcinoma samples using the HTG EdgeSeq Precision Immuno-Oncology Panel. Ingenuity pathway analysis was performed to understand the immunobiology, signaling, and functional perturbations during tumor development.

The samples were divided into 3 groups: 21 SNUCs and SMARC-deficient sinonasal carcinomas; 5 high-grade neuroendocrine carcinomas (HGNECs), with small cell and large cell variants; and 4 high-grade sinonasal carcinomas (HGSNCs) of mixed histology (1 NUT carcinoma, 1 teratocarcinosarcoma, and 2 sinonasal adenocarcinomas). PRAME and ASCL1 emerged as upregulated transcripts with strong protein validation for SNUC and HGNEC; other upregulated candidates EZH2 and BRCA1 offer consideration for alternative targeted therapy, and downregulation of major histocompatibility complex molecules and chemokines represent another hurdle in the development of effective immunotherapy.

This immune-oncology gene expression analysis of 3 groups of high-grade sinonasal carcinoma with emphasis on SNUC identified a number of differentially expressed transcripts reflecting effects on tumorigenesis. Identification of immune pathways should be further investigated for possible integration of immunotherapy into a multidisciplinary approach to these cancers and personalized treatment.

Introduction

The skull base is the location of a wide variety of benign and malignant tumors. The diversity of these histogenetically and biologically heterogeneous neoplasms of ectodermal, endodermal, and mesodermal origins is partly due to the anatomic complexity and highly varied tissues in this compact area[1]. The majority of tumors at these locations are malignant, the most common being tumors of the maxillary sinus (60%), nasal cavity (22%), and ethmoid sinus (15%) and the least common tumors of the frontal and sphenoid sinuses (3%). The most common types of malignancies in the skull base are carcinomas (50%),

followed by mesenchymal tumors (30%), neuroectodermal tumors (15%), and miscellaneous entities (5%)[1; 2; 3]. Sinonasal malignancies have shown dramatic improvement in patient survival, from 20% in the 1950s to 60–80% at the present time [2]. The improvement is tied to the development and use of modern diagnostic tools such as routine office endoscopy and high resolution imaging; improved therapy such as modern skull base surgical techniques of resection and reconstruction, conformal radiation therapy, and more effective systemic therapy; and to improved pathological analysis. Novel diagnostic markers for skull base tumors are reported at a high pace rate, along with increasing evidence justifying the importance of immunophenotyping and genotyping for differentiating among these neoplasms[1; 2; 3]. In a 1973-2006 review of the SEER database, there was a striking difference in five-year relative survival ranging from 30-35% for mucosal melanoma and SNUC to 60-70% for olfactory neuroblastoma, adenoid cystic carcinoma and adenocarcinoma[4]. The prognosis of certain tumors is tied to tumor grade, with a three year survival close to 20% for high-grade carcinomas. The chapter of nasal and paranasal tumors in the World Health Organization 4th edition of Classification of Head and Neck Tumors lists under the umbrella of high-grade carcinomas sinonasal undifferentiated carcinoma (SNUC), SMARCB1-deficient carcinomas, NUT carcinoma, high-grade neuroendocrine carcinoma, sinonasal nonintestinal-type adenocarcinoma, teratocarcinosarcoma [5].

SNUC, a “high-grade epithelial neoplasm of the nasal cavity and paranasal sinuses of uncertain histogenesis with or without neuroendocrine differentiation but without evidence of squamous or glandular differentiation”[6], typically presents with locally extensive disease[5], notoriously refractory to therapy and has a poor prognosis, particularly when the tumor transgresses the cranial base[2; 5; 7; 8]. A subset of sinonasal carcinomas with basaloid/ rhabdoid tumor morphology and loss of expression of SMARCB1 (INI1) and SMARCA4[3; 5; 9; 10], warrant inclusion as a separate new entity among the existing high-grade sinonasal neoplasms[5]. Distinguishing these tumors from the other types of sinonasal malignancies is important because SMARCB1 deficiency may provide a new target for novel treatment approaches that may ultimately lead to improved patient survival[3].

NUT carcinomas are rare, clinically aggressive carcinomas that are characterized by a translocation involving the *NUT* gene on chromosome 15q14 and, in most cases, the bromodomain-containing 4 (*BRD4*) gene on chromosome 19p13.1, resulting in a *BRD4-NUT* fusion gene[5; 11; 12]. In view of the

anecdotal favorable responses of NUT malignancies to certain treatment regimens, including chemotherapy according to Ewing sarcoma protocols or docetaxel and radiotherapy, the distinction of NUT carcinomas from other sinonasal carcinomas appears to be of clinical relevance[11; 12].

Sinonasal tumors with neuroendocrine differentiation represent 5% of all sinonasal malignancies, and the correct classification of these tumors is fundamental for initiating an appropriate treatment strategy[8; 13; 14]. Tumor behavior varies within the spectrum of sinonasal tumors with neuroendocrine differentiation, and a broad distinction should be made between tumors of neuroectodermal origin (e.g., olfactory neuroblastoma [ONB]) and those of epithelial origin (e.g., sinonasal neuroendocrine carcinoma [SNEC])[8; 13; 14]. For ONB, a well-defined treatment strategy consisting of surgery with or without postoperative radiotherapy is the current standard of care, with a reasonable outcome[8; 13; 14]. For SNECs, no clear guidelines are available and treatment outcomes remain variable and poor; several studies have shown large differences in response to treatment and prognosis between the various subtypes of SNEC and SNUC[8; 15; 16]. The head and neck neuroendocrine carcinoma (NEC) classification mirrors that of its counterparts in the respiratory system. These are divided into well-differentiated (carcinoid tumor), moderately differentiated (atypical carcinoid tumor), and poorly differentiated NEC on the basis of cytologic features, mitotic count, and the presence of necrosis. The latter are further divided into large cell NEC (LCNEC) and small cell NEC (SmCNEC)[5; 13]. In the head and neck region, LCNEC comprises two distinct types: (1) tumors composed of large undifferentiated cells with only immunohistochemical or ultrastructural evidence of neuroendocrine differentiation equivalent to SNUC and (2) tumors consisting of large cells arranged in organoid nests, trabeculae, and rosettes and with peripheral palisading of tumor cell nuclei[5; 13].

High-grade nonintestinal sinonasal adenocarcinomas are a wastebasket tumors that cannot be classified as salivary neoplasms, lack an intestinal phenotype, and have moderate to marked cytologic pleomorphism, brisk mitotic count and necrosis. Teratocarcinosarcomas of sinonasal/ head and neck region are heterogeneous uncommon malignancies combining epithelial, primitive neuroepithelial and mesenchymal components. These tumors show a male predominance and affect adults age 18-80 years; the average survival time is less than 2 years, with uncontrolled local recurrences and cervical

metastasis. Recent findings suggest that SMARCA4 inactivation may be a dominant genetic event in teratocarcinosarcoma[17].

The need for alternative treatment modalities, including immunotherapy and targeted therapy, is emerging in the context of resistance to chemotherapy and aggressive clinical course in these high-grade sinonasal carcinomas. The aim of this study was to interrogate and expand the understanding of the tumor immune contexture in high-grade sinonasal carcinomas, with an emphasis on SNUCs, using a specific set of probes targeting 1392 representative immunological RNA transcript targets.

Journal Pre-proof

Materials and Methods

Patient Specimens

For this retrospective gene expression analysis, 30 formalin-fixed, paraffin-embedded tumor specimens were obtained from pathology files. The specimens were collected via biopsy or surgery performed at The University of Texas MD Anderson Cancer Center between 2005 and 2019 from 30 patients with treatment-naïve, high-grade sinonasal carcinomas. All of the specimens were re-reviewed by a head and neck pathologist to confirm the tumor histology and grade. MD Anderson Cancer Center Institutional Review Board approval was obtained prior to the start of the study.

RNA Expression Analysis

Macrodissections of 5 micrometer FFPE sinonasal carcinoma specimens and neighboring normal tissues were lysed using HTG Lysis Buffer, followed by proteinase K digestion, and then transferred to an HTG EdgeSeq platform (HTG Molecular Diagnostics, Inc., Tucson, AZ). On the automated HTG EdgeSeq system, a quantitative nuclease protection assay (qNPA from HTG) was performed. For this, the HTG EdgeSeq Precision Immuno-Oncology Panel (PIP_P38) with 1410 DNA nuclease protection probes (NPPs), was added in excess to the processed sample lysate solutions. The NPPs of PIP_P38 consisted out of single-stranded (ss) DNA oligonucleotide sequences complementary to the mRNA sequences of 1392 genes related to tumor-immune interaction, 10 housekeeping control genes, four negative and positive process controls, and included double stranded (ds) sequencing adapter sequences at both ends. These NPPs were hybridized to their target RNAs producing dsDNA-RNA hybrids. S1 nuclease was added to specifically digest all remaining single stranded nucleic acid chains from excess DNA probes (NPPs) and sample RNAs. S1 nuclease was deactivated, dsDNA-RNA hybrids were melted into single strands, and ssRNA degraded. The resulting DNA probes were quantitatively amplified with polymerase chain reaction adding extended primers (including sequencing primer and sample barcode sequences) for library preparation using KAPA Library Quantification Kit for Illumina Platforms (Roche Sequencing and Life Science, Kapa Biosystems, Wilmington, MA). Library samples were cleaned up to remove excess primers, quantitated, pooled and sequenced using Illumina MiSeq bench top sequencer

(Illumina, San Diego, CA) as part of the HTG EdgeSeq system. HTG Edge host and parser software processed the quantitative sequence data in FASTQ format and produced the gene expression data of our samples in an HTG sample sheet format, which is provided with sample identifications in S-Tab1. All RNA sequencing data are available for download from the National Center for Biotechnology Information (NCBI) Sequence Read Archive (reference PRJNA644026; NCBI, National Institutes of Health, Bethesda, Maryland).

Gene Expression Data Analysis

The software platform HTG EdgeSeq Reveal was used for data analysis. This included determination of differential gene expressions between the group of six normal samples and each of the three groups of sinonasal undifferentiated carcinoma (SNUC), high-grade neuroendocrine carcinoma (HGNEC), and high-grade sinonasal carcinoma (HGSNC). For these comparisons, the algorithm package DESeq2 (<https://bioconductor.org/packages/release/bioc/vignettes/DESeq2/inst/doc/DESeq2.html>) was used and resulted S-Tab2. To find differentially expressed genes with importance in these three study groups, cut-off values of foldchange greater 2 ($FC > 2$) and false discovery rates smaller 0.17 ($FDR < 0.17$) were applied and considered significant for each gene; the resulting table is provided in S-Tab3 and was used for all subsequent analyses.

Pathway Analysis

Computational pathway core analyses and network analyses of the RNA differential expression data of the tumor subtypes were performed using the program Ingenuity Pathway Analysis (IPA; QIAGEN Silicon Valley, Redwood, CA) to identify disease associations, pathway networks, and biomarkers among the genes and noncoding transcripts specific for SNUCs, HGNECs and HGSNCs.

Immunohistochemical Analysis

Immunohistochemical analysis was performed with antibodies against human PRAME (AbCam, Cambridge, MA, dilution 1:100), MASH1 (Novocastra, Newcastle, UK, dilution 1:100), INSM1 (Novus Biologicals, Centennial, CO, dilution 1:100), and PARP1 (Novocastra, Newcastle, UK, dilution 1:100). For

PRAME, immunopositivity was defined as any expression within tumor cells and the location of the staining (nuclear and/or cytoplasmic) was recorded. For MASH1, INSM1 and PARP1 proteins, the nuclear staining results were categorized as positive ($\geq 5\%$ of the area of the entire tissue specimen was stained positive; subcategorized as focal, 5-10%; patchy, 10-50%; or diffuse, $>50\%$) or negative ($<5\%$ of the entire tissue specimen was stained positive).

RESULTS

Patient Characteristics

Clinical characteristics of the 30 patients are depicted in Table 1. The cohort included a spectrum of high-grade sinonasal carcinomas and was divided into 3 groups. SNUCs were the most represented in group (A), with 15 primary SNUCs, 1 SNUC liver metastasis, 1 *SMARCB1*-deficient sinonasal carcinoma, and 1 *SMARCA4*-deficient sinonasal carcinoma); HGN ECs (group B) included 3 small cell type and 2 large cell type NECs, and HGSNCs were a mix of 1 each of the following: NUT carcinoma, teratocarcinosarcoma, sinonasal adenocarcinoma oncocytic type, and sinonasal carcinoma with extensive blastemal component. Age at diagnosis ranged from 25 to 82 years. Most patients were male (70%). The nasal cavity and maxillary sinus were the most common primary subsites ($n = 14$ and $n = 11$, respectively). Locally advanced stages—mainly advanced T4a—were prevalent. Treatment consisted of surgical resection (followed by radiation with or without concurrent chemotherapy) or curative chemoradiotherapy (preceded by induction chemotherapy). No difference in treatment was observed among the histotypes. Follow-up intervals ranged from 9 to 83 months. At the last encounter, 11 patients had no evidence of disease, 3 were alive with disease, and 10 had died of disease; 2 patients died of unrelated causes; and for 4 patients, follow-up information was not available.

Histopathological Characteristics

Representative morphologic characteristics per subgroup are illustrated in Figures 1-4. One histological observation was that the stromal immune infiltrate was variable, with several of the SNUCs showing

inflamed stroma with a mix of acute and chronic inflammatory infiltrate (immunologically “hot” tumors) and other carcinomas lacking histological evidence of immune infiltrate/response (“cold” or excluded tumors). Mast cells were noted in several of the SNUC cases (Figure 1). Tertiary lymphoid structures were not appreciated in any of the examined cases. Next-generation sequencing using the CLIA in-house platform OncoPrint (OCPv3, ThermoFisher, which detects somatic mutations in the coding sequence of 134 genes and selected copy number variations/ amplifications in 47 genes, overlap: 146 genes total) revealed that cases 17 and 19 had IDH2 somatic mutations. Immunohistochemistry performed on SNUCs using an anti-IDH1/2 mutant (R132/172) antibody found immunoreactivity in 11 of the tested SNUCs (including those cases with OncoPrint validation), whereas the NECs and olfactory neuroblastoma tested were negative.

Case 24 morphologically and phenotypically fit in the category of SmCNEC (Figure 3). Among the pathologically challenging cases was case 27, which was originally called an ameloblastic carcinoma before being reclassified as a NUT carcinoma (NUT over. confirmed by NGS) (Figure 4a). NGS using OncoPrint assays picked up *NOTCH2* and *FANCI* somatic mutations in the teratocarcinoma (TCS) (Figure 4b); TCS was negative for SMARCB1 and SMARCA4. This reinforces the diagnostic challenge of some of the high-grade sinonasal carcinomas, with high rates of discrepancies and the value of a second subspecialized pathology expert opinion. In our institutional experience approximately 25% of the outside referrals of sinonasal pathology were reclassified after review by head and neck pathologists. Cases 29 and 30 were both classified under the umbrella of sinonasal adenocarcinomas non-intestinal type (Figures 4c-4d). The sinonasal adenocarcinoma oncocytic variant (case 29, Figure 4c) had a significant component of papillary structures; fluorescence in situ hybridization was “indeterminate” for *ETV6* and negative for *RET* rearrangement. A high-grade blastema component dominated the morphology of case 30 (Figure 4d).

Transcriptomes of Immuno-Oncology related Genes

From 21 SNUCs, 5 HGNECs, and 4 HGSNCs RNA expression profiles of 1392 genes, related to tumor-immune interaction (HTG immuno-oncology panel PIP_P38), were generated and compared to normal sinonasal mucosal samples, and with each other. Differentially expressed genes, in comparison to normal

samples, with FC values greater than 2, and FDR values smaller than 0.17, yielded for the SNUCs, 254 genes and noncoding transcripts (167 upregulated and 87 downregulated), for the HGNECs, 387 genes and noncoding transcripts (230 upregulated and 157 downregulated), and for the HGSNCs, 331 genes and noncoding transcripts, with 161 upregulated and 170 downregulated (S-Tab3). The top 10 specific genes differentially expressed between HGNECs and SNUCs (A- upregulated; B- downregulated) and between HGSNCs and SNUCs (C- upregulated, D- downregulated) are presented in Figure 5. *PRAME* with fold change (FC) 8.4 was the top upregulated gene for SNUCs, followed by cellular assembly and organization genes *FN1* (FC: 6.6), *CEP55* (FC: 4.9), *COL1A* (FC: 4.8), *PLSG3* (FC: 4.7), and chemokine family members *CXCL8* (FC: 4.7), *CXCL5* (FC: 4.5). Although not among the top upregulated genes, *ETV4* (FC: 3.4), *BRCA1* (FC: 3.1), and *EZH2* (FC: 2.6) were also found to be upregulated in the SNUC group. The neuroendocrine family genes *CHGA1* (FC: 20.5) and *ASCL1* (FC: 18.8) had the highest values among the HGNECs, followed by *CXCL5* (FC: 18.6), *SPOA8* (FC: 17.5), *SPP1* (FC: 14.8), serpin family genes B2, B5 (FC: 9.5, 9.2), and keratin 16 genes (FC: 8.9) dominated the HGSNCs. *DMBT1* and lysozyme *LYZ* were the most consistently downregulated genes in all three groups. Of interest, major histocompatibility complex (MHC) class I and II members were also downregulated, along with several other chemokine family members (including CCL28 and CCL14). Complete lists of all genes and differential expressions are provided in supplemental Tables S1 to S3.

Pathway Analysis

IPA revealed a number of immune-related functional categories to be differentially expressed in sinonasal carcinomas compared to normal sinonasal mucosa. Movement of myeloid cells and chemotaxis were upregulated, while several other genes involved in chemotaxis were downregulated in carcinomas compared to normal tissue. The top networks with differentially expressed transcripts and genes specific for SNUC were those associated with cancer, cell cycle, cellular assembly and organization, cellular function and maintenance, humoral immune responses, and protein synthesis. Deregulated top networks of HGNECs were TRIM45 related pathways of innate immune system and interferon gamma signaling, and networks involved in regulation of natural killer cells, apoptosis, carcinogenesis, invasion, and proliferation of tumor cells. Figure 6 illustrates representative networks for SNUCs and HGNECs.

Biomarker Analysis

To validate the differential RNA transcription results, and to find potential biomarkers, we used immunohistochemical analysis to assess the protein expression of the most upregulated genes using the following antibodies: PRAME (for SNUC), MASH1, INSM1, and PARP1 (for HGNEC). PRAME showed expression in 17 of 19 tested SNUCs (Figure 1). Although naïve tumors were the focus of the transcriptome, we had the opportunity of analyzing a post-induction resected surgical specimen (case 1). There was an enhanced inflammatory response (Figure 1b- C). PRAME was detected by immunohistochemistry, however at lower protein levels compared to naïve SNUC (Figure 1b- D). Unrelated to the current topic, but of interest for ongoing and future work, the post-induction SNUC showed ability of forming tumor spheroids that maintained tumoral morphology (Figure 1b-E, F). The authenticated cell line (previously published[18]) also showed mRNA PRAME; the protein level was barely detected with frequent passages of the cell line (Figure 1b-G, H). PRAME expression was detected in one LCNEC (case 22). All HGNEC samples expressed the neuroendocrine markers MASH1, INSM1, and PARP1 (representative illustrations are shown in Figure 3).

DISCUSSION

Given the rarity of sinonasal carcinomas the transcriptomic data are scarce. This work focused primarily on the SNUCs, highlighting a number of key signaling networks; other representative carcinomas with high-grade histologies (HCNECs and HGSNCs) were analyzed in parallel.

Our global analyses revealed the enrichment of gene signatures indicative of carcinogenesis, cell cycle, cellular assembly and organization, cellular function and maintenance, and humoral immune responses in sinonasal carcinomas.

Within the past few decades many tumor-specific antigens (TSAs) and tumor-associated antigens (TAAs) have been discovered [19; 20; 21; 22; 23]. TSAs may result from gene mutations or from the expression of alternative open reading frames, resulting from chromosomal rearrangements[20; 22; 24; 25]; normal tissues frequently carry TAAs, with the drawback of autoimmunity development in parallel to breaking tolerance to these antigens through vaccination and tumor recognition [20; 21; 25; 26].

PRAME (FC 8.40) was the top upregulated gene in SNUCs, and FC half values (4.8, position 47) were seen within HGNECs but not detected within HGSNCs. PRAME (preferentially expressed antigen in melanoma) is a testis-selective cancer antigen with restricted expression in somatic tissues and re-expression in various cancers. PRAME has gained interest as a candidate target for immunotherapy[27; 28]. The cellular and molecular functions of PRAME in normal and neoplastic cells remain largely unclear and may differ depending on tissue specificity and/or the subcellular localization of PRAME[27; 28]. PRAME plays a role in the acquisition of various cancer hallmarks, including replicative immortality or stemness, invasion, and metastasis[27; 28]. In addition to supporting tumor features, PRAME has been implicated in the regulation of the immune response[27; 29; 30; 31].

ASCL1 (Aschaete-scute homolog 1, *mASH*) and *CHGA1* (chromogranin) had the highest values among the HGNECs and were entirely specific to this group; *INSM1* (insulinoma-associated 1) and *NKX2-1* followed. All 5 HGNECs expressed MASH1 and INSM1 protein levels. Only a few studies have addressed the expression pattern of *mASH1* in neoplastic tissues[32; 33; 34; 35]. In a study by Atree-Tacha et al.[36], *mASH1* proved relatively specific for high-grade pulmonary NECs, being reactive in 66.7% of LCNECs and 82.5% of SmCNECs but less specific for low-grade (0%) and intermediate-grade (42.9%) tumors, staining fewer than 2% of non-neuroendocrine lung carcinomas. The authors argued that MASH1 could be used as a marker to distinguish high-grade NEC from carcinoid tumors and non-neuroendocrine neoplasms[36]. *ASH1* is a useful marker for cancers with neuroendocrine features, as it has been documented as a key player in modulating neuroendocrine differentiation in tumor cells[34]. *ASH1* expression levels are inversely associated with the degree of tumor differentiation (high-grade tumors show increased expression of protein), which correlates well with studies indicating that expression of *ASH1* appears to be restricted to immature cells[32; 33; 34; 37]. Prior work from our group[35] showed expression of MASH1 in high-grade neuroendocrine tumors (SmCNECs, LCNECs, and high-grade ONBs), with absent or modest levels in well-differentiated counterparts (low-grade olfactory neuroblastoma and carcinoids).

The nomenclature of LCNEC is controversial among head and neck pathologists, however, it is our opinion and others, that in the sinonasal area undifferentiated carcinoma can be viewed as large cell carcinoma with or without evidence of neuroendocrine differentiation. This contention is clinically

supported by our experience with sinonasal malignancies: looking at the overall survival (OS) and progression-free survival (PFS), low-grade ONBs stand out with the best outcomes, while high-grade NECs, mostly the small cell variant, carry worse outcomes; clinical outcomes for SNUCs, large cell NECs and high-grade ONBs cluster together in the middle[16]. Similarly, the concept of “olfactory carcinoma” as an overlap of large cell neuroendocrine carcinoma/ SNUC, ONB and sinonasal adenocarcinoma has to be revisited in the context of anatomic location. Case 22 was classified as LCNEC (morphologically and phenotypically), but within the anatomic boundaries of the cribriform plate and upper nasal vault, the terminology of olfactory carcinoma may gain more recognition among experts. In our experience (unpublished data) we found all low-grade ONBs to be positive for Somatostatin Receptor 2 (STR2) while high-grade ONBs and high-grade NECs did not express STR2. This raises the possibility of using STR2 as an adjunct diagnostic biomarker for sinonasal neuroendocrine tumors particularly on small biopsies.

MHC class I and class II molecules were both found to be downregulated in SNUCs (HLA-E, FC: -2.11 and HLA-DOB, FC: -2.33), HGNECs (HLA-DMA, FC: -2.09), and HGSNCs (HLA-G, FC: -2.35; HLA-DOB, FC: -3.71; HHLA2, FC: -17.59). Similarly, downregulated values were found for the transport family member ABCB1 (ATP binding cassette subfamily B1 member) in SNUCs and HGNECs (FCs: -2.11 and -2.49, respectively).

The interplay between immune and tumor cells is complex[20; 25]. Because many tumors downregulate the expression of MHC molecules, the immune system could play a role in controlling the progression and evolution of cancer. MHC class I antigen presentation is often affected in human cancers, and the capacity to induce upregulation of MHC class I cell surface expression is a critical step in the induction of tumor rejection. It is well established that tumor immune escape is associated with MHC class I downregulation, as seen in different human and experimental tumors and reviewed in many previous reports[38; 39; 40]. The genetic diversity at the MHC class I and II loci is another hurdle in the development of effective immunotherapy[19; 38; 39; 40; 41].

Several of the SNUCs in this study showed mixed inflammatory infiltrates with eosinophils and neutrophils (Figure 1). It is well established that tumor-infiltrating immune cells play critical roles in the pathogenesis of various cancers. Our data highlighted the presence of a gene signature indicative of altered immune infiltration. Interestingly, we found that *CXCL8* and *CXCL5* were upregulated in high-grade sinonasal

carcinomas. Expression of CXCL5 has been observed in eosinophils and can be inhibited with IFN- γ . CXCL5 has also been described to regulate neutrophil homeostasis, and several studies have speculated that CXCL5 is a potential therapeutic target for the restriction of pathogenic neutrophil infiltration in Th17-mediated autoimmune diseases while leaving intact the neutrophil function of protective immunity against invading pathogens[42]. The protein encoded by CXCL8 is secreted primarily by neutrophils, where it serves as a chemotactic factor by guiding the neutrophils to the site of infection; this chemokine is also a potent angiogenic factor. Altered chemokine expression in the tumor microenvironment results in leukocyte activation and trafficking, angiogenesis, metastasis, and proliferation of cancer cells. In cancer patients, CXCL8 expression might be used to assess the patient's prognosis and response to chemotherapy. In various types of cancer, high levels of CXCL8 in serum or at local sites correlate with aggressive disease and poor initial response to oxaliplatin, 5-fluorouracil, and paclitaxel. On the other hand, several chemokines such as CCL28 and CCL14 were downregulated in SNUCs and HGNECs compared to normal tissue. The cytokine encoded by the *CCL28* gene displays a strong homing capability for B and T cells at several mucosal and epithelial sites and orchestrates the trafficking and functioning of lymphocytes; several studies have referred to the dual properties of *CCL28* and its role as an anchoring point in bridging the innate and adaptive immunity[43]. CCL14 activates monocytes but does not induce their chemotaxis. This may explain why the infiltration of monocytes and T and B cells is relatively scarce in sinonasal carcinomas. Targeting migration-related chemokines and their receptors in sinonasal tumors might be beneficial for immunotherapy.

The gene deleted in malignant brain tumors *DMBT1*, and lysozyme *LYZ* were consistently found to be the most downregulated genes in all 3 groups of high-grade sinonasal carcinomas. *DMBT1* has been proposed as a candidate tumor suppressor in brain, gastrointestinal, lung and oral squamous cell carcinoma[44; 45; 46; 47]. It codes for a protein of unknown function belonging to the superfamily of scavenger receptor cysteine-rich proteins (*SCRs*); *SCRs* are implicated in functions within the immune system and considered to be involved in host defense by pathogen binding. *LYZ* is an antimicrobial enzyme that is part of the innate immune system.

EZH2 (enhancer of zeste homolog 2), a histone methyltransferase that catalyzes tri-methylation of histone H3 at Lys27 (H3K27me3) to regulate gene expression through epigenetic mechanisms, was

found to be moderately upregulated in SNUCs and HGNECs (FC: +2.55 and +3.90, respectively). *EZH2* interacts with both histone and non-histone proteins to regulate expression of downstream genes, affecting several physiological functions including cancer progression, malignancy, and drug resistance[48; 49]. *EZH2*-dependent repression of p16/CDKN2A results in cell cycle progression in multiple cancers. Therefore, *EZH2* is a potential target for cancer therapy and a variety of inhibitors have been developed[48; 49]. Cancers harboring *SWI/SNF* mutations and gain-of-function *EZH2* mutations confer dependency on *EZH2* inhibitors; pre-clinical evidence suggests a potential benefit of combination therapy with an *EZH2* inhibitor[48; 50]. At least in the case of cancers driven by *SWI/SNF* mutation, Ras pathway mutations confer resistance to *EZH2* inhibitors[48; 49; 51].

BRCA1 was another moderately upregulated gene in SNUCs and HGNECs. This signature is linked to defects in homologous recombination, which is a vulnerability that might be exploited by treatment with PARP inhibitors based on the principle of synthetic lethality. All HGNECs expressed high levels of PARP1 at the protein level (Figure 2). Expression of PARP1 on immunohistochemical analysis is currently being explored to select patients who are likely to benefit from PARP inhibitors[52; 53; 54].

Our study is in an exploratory phase and there are several limitations. The sample numbers were relatively small, and the majority of the analyzed samples were derived from diagnostic biopsies, in an effort to assess naïve tumors; thus the issue of tumor heterogeneity may have been unrecognized to a certain extent. The transcriptome analysis we employed focused on an immune-oncology related panel of 1392 genes, which compared to unbiased whole transcriptome expression analysis constituted a strong limitation. This platform was chosen owing to its ability to analyze the very small FFPE tissue quantities available to us.

The current work aimed to interrogate the immune environment and emerging biomarkers in high-grade sinonasal carcinomas, with an emphasis on SNUC. Further studies of whole transcriptome analyses and multiplex immunostainings will answer the questions raised by the preliminary data generated here. To our knowledge, this is the first description of PRAME having preferential expression in SNUCs, opening an avenue for further investigations of PRAME as a biomarker (in larger annotated multi-institutional cohorts), and functional studies addressing the immunogenicity and safety of PRAME

immunotherapeutics. Profiling and spatial analysis of tumor immune microenvironment are our immediate goals.

In conclusion, the immune-oncology gene expression analysis identified specific profiles of differentially expressed transcripts exerting their effects on tumorigenesis. The characteristic genes and proteins discovered for these sinonasal carcinoma histotypes with their genomic pathways generated potential candidates for disease biomarkers and therapeutic opportunities, like PRAME promoting undifferentiated cell states in SNUCs, and ASCL1 a neuronal-specific transcription factor involved in neuroendocrine differentiation in HGNEC. Especially the implied deregulated immune pathways of humoral immune response in SNUCS, and the TRIM45 related pathways of innate immune system and interferon gamma signaling in HGNEC, need to be further investigated for possible integration of immunotherapy into a multidisciplinary and/or personalized approach for treating these cancers.

Declaration

Funding: This work was supported by MD Anderson Cancer Center research funds (Dr. Diana Bell).

Conflict of Interest/ Competing Interest: The authors declare that they have no conflict of interest.

Ethics approval: The use of patient samples and the data inquiry were approved by the MD Anderson Cancer Center Institutional Review Committee.

Consent to participate: N/A

Consent for publication: N/A

Author's contributions: Drs. Bell had full access to all the data and take responsibility for the integrity of the data and the accuracy of the analysis. Concept and design: Bell, Hanna. Acquisition, analysis, or interpretation of data: All authors. Drafting of the manuscript: Bell. Critical revision of the manuscript for important intellectual content: All authors.

References

- [1] D. Bell, and E.Y. Hanna, Sinonasal undifferentiated carcinoma: morphological heterogeneity, diagnosis, management and biological markers. *Expert Rev Anticancer Ther* 13 (2013) 285-96.
- [2] A.S. Abdelmeguid, D. Bell, and E.Y. Hanna, Sinonasal Undifferentiated Carcinoma. *Curr Oncol Rep* 21 (2019) 26.
- [3] A. Agaimy, A. Franchi, V.J. Lund, A. Skalova, J.A. Bishop, A. Triantafyllou, S. Andreasen, D.R. Gnepp, H. Hellquist, L.D.R. Thompson, A. Rinaldo, and A. Ferlito, Sinonasal Undifferentiated Carcinoma (SNUC): From an Entity to Morphologic Pattern and Back Again-A Historical Perspective. *Adv Anat Pathol* 27 (2020) 51-60.
- [4] J.H. Turner, and D.D. Reh, Incidence and survival in patients with sinonasal cancer: a historical analysis of population-based data. *Head Neck* 34 (2012) 877-85.
- [5] A.K. El-Naggar, J.K.C. Chan, J. Rubin Grandis, T. Takata, P.J. Slootweg, and C. International Agency for Research on, WHO classification of head and neck tumours, 2017.
- [6] H.F. Frierson, Jr., S.E. Mills, R.E. Fechner, J.B. Taxy, and P.A. Levine, Sinonasal undifferentiated carcinoma. An aggressive neoplasm derived from Schneiderian epithelium and distinct from olfactory neuroblastoma. *Am J Surg Pathol* 10 (1986) 77-9.
- [7] M. Amit, A.S. Abdelmeguid, T. Watcherporn, H. Takahashi, S. Tam, D. Bell, R. Ferrarotto, B. Glisson, M.E. Kupferman, D.B. Roberts, S.Y. Su, S.M. Raza, F. DeMonte, and E.Y. Hanna, Induction Chemotherapy Response as a Guide for Treatment Optimization in Sinonasal Undifferentiated Carcinoma. *J Clin Oncol* 37 (2019) 504-512.
- [8] S.Y. Su, D. Bell, and E.Y. Hanna, Esthesioneuroblastoma, neuroendocrine carcinoma, and sinonasal undifferentiated carcinoma: differentiation in diagnosis and treatment. *Int Arch Otorhinolaryngol* 18 (2014) S149-56.
- [9] J.A. Bishop, Recently described neoplasms of the sinonasal tract. *Semin Diagn Pathol* 33 (2016) 62-70.
- [10] J.A. Bishop, C.R. Antonescu, and W.H. Westra, SMARCB1 (INI-1)-deficient carcinomas of the sinonasal tract. *Am J Surg Pathol* 38 (2014) 1282-9.
- [11] C.A. French, NUT midline carcinoma. *Cancer Genet Cytogenet* 203 (2010) 16-20.
- [12] C.A. French, NUT Carcinoma: Clinicopathologic features, pathogenesis, and treatment. *Pathol Int* 68 (2018) 583-595.
- [13] D. Bell, Sinonasal Neuroendocrine Neoplasms: Current Challenges and Advances in Diagnosis and Treatment, with a Focus on Olfactory Neuroblastoma. *Head Neck Pathol* 12 (2018) 22-30.
- [14] D. Bell, E.Y. Hanna, R.S. Weber, F. DeMonte, A. Triantafyllou, J.S. Lewis, Jr., A. Cardesa, P.J. Slootweg, G. Stenman, D.R. Gnepp, K.O. Devaney, J.P. Rodrigo, A. Rinaldo, B.M. Wenig, W.H. Westra, J.A. Bishop, H. Hellquist, J.L. Hunt, K. Kusafuka, B. Perez-Ordóñez, M.D. Williams, R.P. Takes, and A. Ferlito, Neuroendocrine neoplasms of the sinonasal region. *Head Neck* 38 Suppl 1 (2016) E2259-66.
- [15] E.H. Mitchell, A. Diaz, T. Yilmaz, D. Roberts, N. Levine, F. DeMonte, E.Y. Hanna, and M.E. Kupferman, Multimodality treatment for sinonasal neuroendocrine carcinoma. *Head Neck* 34 (2012) 1372-6.
- [16] D.I. Rosenthal, J.L. Barker, Jr., A.K. El-Naggar, B.S. Glisson, M.S. Kies, E.M. Diaz, Jr., G.L. Clayman, F. Demonte, U. Selek, W.H. Morrison, K.K. Ang, K.S. Chao, and A.S. Garden, Sinonasal malignancies with neuroendocrine differentiation: patterns of failure according to histologic phenotype. *Cancer* 101 (2004) 2567-73.
- [17] L.M. Rooper, N. Uddin, J. Gagan, L.A.A. Brosens, K.R. Magliocca, M.A. Edgar, L.D.R. Thompson, A. Agaimy, and J.A. Bishop, Recurrent Loss of SMARCA4 in Sinonasal Teratocarcinosarcoma. *Am J Surg Pathol* (2020).

- [18] Y. Takahashi, M.E. Kupferman, D. Bell, T. Jiffar, J.G. Lee, T.X. Xie, N.W. Li, M. Zhao, M.J. Frederick, A. Gelbard, J.N. Myers, and E.Y. Hanna, Establishment and characterization of novel cell lines from sinonasal undifferentiated carcinoma. *Clin Cancer Res* 18 (2012) 6178-87.
- [19] M. Canning, G. Guo, M. Yu, C. Myint, M.W. Groves, J.K. Byrd, and Y. Cui, Heterogeneity of the Head and Neck Squamous Cell Carcinoma Immune Landscape and Its Impact on Immunotherapy. *Front Cell Dev Biol* 7 (2019) 52.
- [20] O.J. Finn, Cancer immunology. *N Engl J Med* 358 (2008) 2704-15.
- [21] O.J. Finn, Human Tumor Antigens Yesterday, Today, and Tomorrow. *Cancer Immunol Res* 5 (2017) 347-354.
- [22] O.J. Finn, Introduction to the special issue: Tumor antigens in the time of the coronavirus pandemic. *Semin Immunol* 47 (2020) 101396.
- [23] O. Palata, N. Podzimkova Hradilova, D. Mysikova, B. Kutna, H. Mrazkova, R. Lischke, R. Spisek, and I. Adkins, Detection of tumor antigens and tumor-antigen specific T cells in NSCLC patients: Correlation of the quality of T cell responses with NSCLC subtype. *Immunol Lett* 219 (2020) 46-53.
- [24] L. De Cecco, M.S. Serafini, C. Facco, R. Granata, E. Orlandi, C. Falla, L. Licitra, E. Marchesi, F. Perrone, S. Pilotti, P. Quattrone, C. Piazza, F. Sessa, M. Turri, Zanoni, P. Battaglia, P. Castelnuovo, P. Antognoni, S. Canevari, and P. Bossi, A functional gene expression analysis in epithelial sinonasal cancer: Biology and clinical relevance behind three histological subtypes. *Oral Oncol* 90 (2019) 94-101.
- [25] O.J. Finn, Immuno-oncology: understanding the function and dysfunction of the immune system in cancer. *Ann Oncol* 23 Suppl 8 (2012) viii6-9.
- [26] O.J. Finn, A Believer's Overview of Cancer Immunological Surveillance and Immunotherapy. *J Immunol* 200 (2018) 385-391.
- [27] G. Al-Khadairi, and J. Decock, Cancer Testis Antigens and Immunotherapy: Where Do We Stand in the Targeting of PRAME? *Cancers (Basel)* 11 (2019).
- [28] Y. Xu, R. Zou, J. Wang, Z.W. Wang, and X. Zhu, The role of the cancer testis antigen PRAME in tumorigenesis and immunotherapy in human cancer. *Cell Prolif* 53 (2020) e12770.
- [29] W. Cai, and H. Yang, The structure and regulation of Cullin 2 based E3 ubiquitin ligases and their biological functions. *Cell Div* 11 (2016) 7.
- [30] T. De Pas, M. Giovannini, M. Roccigno, C. Catania, F. Toffalorio, G. Spitaleri, A. Delmonte, M. Barberis, L. Spaggiari, P. Sciti, G. Veronesi, and F. De Braud, Vaccines in non-small cell lung cancer: rational combination strategies and update on clinical trials. *Crit Rev Oncol Hematol* 83 (2012) 432-43.
- [31] A. Salmaninejad, M.R. Zamani, M. Pourvahedi, Z. Golchehre, A. Hosseini Bereshneh, and N. Rezaei, Cancer/Testis Antigens: Expression, Regulation, Tumor Invasion, and Use in Immunotherapy of Cancers. *Immunol Invest* 45 (2016) 619-40.
- [32] H. Kokubu, T. Ohtsuka, and R. Kageyama, Mash1 is required for neuroendocrine cell development in the glandular stomach. *Genes Cells* 13 (2008) 41-51.
- [33] S. Kudoh, Y. Tenjin, H. Kameyama, T. Ichimura, T. Yamada, A. Matsuo, N. Kudo, Y. Sato, and T. Ito, Significance of achaete-scute complex homologue 1 (ASCL1) in pulmonary neuroendocrine carcinomas; RNA sequence analyses using small cell lung cancer cells and Ascl1-induced pulmonary neuroendocrine carcinoma cells. *Histochem Cell Biol* (2020).
- [34] S. La Rosa, A. Marando, G. Gatti, I. Rapa, M. Volante, M. Papotti, F. Sessa, and C. Capella, Achaete-scute homolog 1 as a marker of poorly differentiated neuroendocrine carcinomas of different sites: a validation study using immunohistochemistry and quantitative real-time polymerase chain reaction on 335 cases. *Hum Pathol* 44 (2013) 1391-9.

- [35] M.W. Taggart, E.Y. Hanna, P. Gidley, R.S. Weber, and D. Bell, Achaete-scute homolog 1 expression closely correlates with endocrine phenotype and degree of differentiation in sinonasal neuroendocrine tumors. *Ann Diagn Pathol* 19 (2015) 154-6.
- [36] D. Altree-Tacha, J. Tyrrell, and F. Li, mASH1 is Highly Specific for Neuroendocrine Carcinomas: An Immunohistochemical Evaluation on Normal and Various Neoplastic Tissues. *Arch Pathol Lab Med* 141 (2017) 288-292.
- [37] S.X. Jiang, T. Kameya, H. Asamura, A. Umezawa, Y. Sato, J. Shinada, Y. Kawakubo, T. Igarashi, K. Nagai, and I. Okayasu, hASH1 expression is closely correlated with endocrine phenotype and differentiation extent in pulmonary neuroendocrine tumors. *Mod Pathol* 17 (2004) 222-9.
- [38] A. Garcia-Lora, I. Algarra, and F. Garrido, MHC class I antigens, immune surveillance, and tumor immune escape. *J Cell Physiol* 195 (2003) 346-55.
- [39] F. Garrido, N. Aptsiauri, E.M. Doorduyn, A.M. Garcia Lora, and T. van Hall, The urgent need to recover MHC class I in cancers for effective immunotherapy. *Curr Opin Immunol* 39 (2016) 44-51.
- [40] B. Seliger, The link between MHC class I abnormalities of tumors, oncogenes, tumor suppressor genes, and transcription factors. *J Immunotoxicol* 11 (2014) 303-10.
- [41] J. Thibodeau, M.C. Bourgeois-Daigneault, and R. Lapointe, Targeting the MHC Class II antigen presentation pathway in cancer immunotherapy. *Oncotarget* 1 (2012) 908-916.
- [42] E.M. Disteldorf, C.F. Krebs, H.J. Paust, J.E. Turner, G. Nourailas, A. Tittel, C. Meyer-Schwesinger, G. Stege, S. Brix, J. Velden, T. Wiech, U. Helmchen, O.M. Steinmetz, A. Peters, S.B. Bannstein, A. Kaffke, C. Llanto, S.A. Lira, H.W. Mittrucker, R. A. Stahl, C. Kurts, S.H. Kaufmann, and U. Panzer, CXCL5 drives neutrophil recruitment in TH17-mediated GN. *J Am Soc Nephrol* 26 (2015) 55-66.
- [43] T. Mohan, L. Deng, and B.Z. Wang, CCL28 chemokine: An anchoring point bridging innate and adaptive immunity. *Int Immunopharmacol* 51 (2017) 165-170.
- [44] M.A. Imai, T. Moriya, F.L. Imai, M. Shiha, H. Bakawa, H. Yokoe, K. Uzawa, and H. Tanzawa, Down-regulation of DMBT1 gene expression in human oral squamous cell carcinoma. *Int J Mol Med* 15 (2005) 585-9.
- [45] J. Mollenhauer, S. Herbertz, U. Holmskov, M. Tolnay, I. Krebs, A. Merlo, H.D. Schroder, D. Maier, F. Breitling, S. Wiemann, H.J. Grone, and A. Poustka, DMBT1 encodes a protein involved in the immune defense and in epithelial differentiation and is highly unstable in cancer. *Cancer Res* 60 (2000) 1704-10.
- [46] M. Mori, T. Shiraishi, S. Tanaka, M. Yamagata, K. Mafune, Y. Tanaka, H. Ueo, G.F. Barnard, and K. Sugimachi, Lack of DMBT1 expression in oesophageal, gastric and colon cancers. *Br J Cancer* 79 (1999) 211-3.
- [47] W. Wu, B.L. Kemp, M.L. Proctor, A.F. Gazdar, J.D. Minna, W.K. Hong, and L. Mao, Expression of DMBT1, a candidate tumor suppressor gene, is frequently lost in lung cancer. *Cancer Res* 59 (1999) 1846-51.
- [48] M. Yamagishi, and K. Uchamaru, Targeting EZH2 in cancer therapy. *Curr Opin Oncol* 29 (2017) 375-381.
- [49] K.S. Yan, C.Y. Lin, T.W. Liao, C.M. Peng, S.C. Lee, Y.J. Liu, W.P. Chan, and R.H. Chou, EZH2 in Cancer Progression and Potential Application in Cancer Therapy: A Friend or Foe? *Int J Mol Sci* 18 (2017).
- [50] A. Italiano, J.C. Soria, M. Toulmonde, J.M. Michot, C. Lucchesi, A. Varga, J.M. Coindre, S.J. Blakemore, A. Clawson, B. Suttle, A.A. McDonald, M. Woodruff, S. Ribich, E. Hedrick, H. Keilhack, B. Thomson, T. Owa, R.A. Copeland, P.T.C. Ho, and V. Ribrag, Tazemetostat, an EZH2 inhibitor, in relapsed or refractory B-cell non-Hodgkin lymphoma and advanced solid tumours: a first-in-human, open-label, phase 1 study. *Lancet Oncol* 19 (2018) 649-659.
- [51] K.H. Kim, and C.W. Roberts, Targeting EZH2 in cancer. *Nat Med* 22 (2016) 128-34.

- [52] A.D. D'Andrea, Mechanisms of PARP inhibitor sensitivity and resistance. *DNA Repair (Amst)* 71 (2018) 172-176.
- [53] M.F. Langelier, T. Eisemann, A.A. Riccio, and J.M. Pascal, PARP family enzymes: regulation and catalysis of the poly(ADP-ribose) posttranslational modification. *Curr Opin Struct Biol* 53 (2018) 187-198.
- [54] R.A. Stewart, P.G. Pilie, and T.A. Yap, Development of PARP and Immune-Checkpoint Inhibitor Combinations. *Cancer Res* 78 (2018) 6717-6725.

Journal Pre-proof

Figure Legends

Figure 1. Sinonasal undifferentiated carcinoma (SNUC)

1a. Case 7. A-E (hematoxylin and eosin; 4x, 10x, 20x magnifications). SNUC infiltrating with nests and trabeculae, in the absence of squamous or glandular differentiation, with stromal desmoplastic stromal response and mixed inflammatory infiltrate. Nuclei are medium to large in size and are surrounded by small amounts of eosinophilic cytoplasm that lacks a syncytial quality; nucleoli are single and prominent. Stromal atypia and scattered mast cells (D, E). Strong tumoral nuclear expression with anti-PRAME immunostaining (F).

1b. Case 1. Naïve SNUC A, B. A-hematoxylin and eosin (4X, 10X). B- PRAME. Post-induction C, D. C-hematoxylin and eosin (4X, 10X)- presence of an enhanced inflammatory response in SNUC. D- PRAME protein at lower levels. D, E- secondary tumor spheroids generated from post-treated surgically resected specimen- maintaining morphological features of SNUC. F, G cytopins preparations from late passage of generated cell line, with low PRAME protein levels (H).

Figure 2. SMARCB1 (INI1)-deficient sinonasal carcinoma

Case 14. A-C (hematoxylin and eosin, 4x, 10x, 20x magnifications). The SMARCB1 (INI1)-deficient carcinomas grow as epithelioid nests in the sinonasal submucosa (A, inset), with stromal inflammatory infiltrate (A, C) and entrapment of the vidian nerve branch (B). Complete loss of SMARCB1 (INI1) immunohistochemical expression (positive staining highlights vessels as internal control) (D) and PRAME expression by the tumor cells (E: PRAME is strongly expressed in the cohesive areas of the carcinoma; F: weaker reactivity of the discohesive rhabdoid tumor cells; E inset: the uninvolved adjacent sinonasal mucosa is negative, with an artifactual apical chromogenic deposition).

Figure 3. High-grade neuroendocrine carcinoma (HGNEC)

Case 24. Small cell neuroendocrine carcinoma. A-C: hematoxylin and eosin (2x, 10x, 20x). D: anti-MASH1; E anti-INSM1, 4x; F anti-PARP1, 4x.

Figure 4. High-grade sinonasal carcinoma (HGSNC)

4a. Case 27. NUT carcinomas. A (hematoxylin and eosin; 0.5 x, 10x). Original biopsy misdiagnosed as ameloblastic carcinoma (basaloid carcinoma, with peripheral cellular palisading and central areas reminiscent of stellate reticulum). B-C (hematoxylin and eosin; 2x, 10x). Resection specimen: high-grade carcinoma composed of undifferentiated basaloid cells with focal, often abrupt, squamous differentiation. Anti-p40 (D) and anti-NUT (E) monoclonal antibodies are strongly positive within the tumor, aiding the diagnosis.

4b. Case 28. Teratocarcinosarcoma. A-F (hematoxylin and eosin; 0.5x, 4x, 10x). High-grade polypoidal malignancy (A) with significant small blue cells/primitive component and associated necrosis and increased apoptosis (B); closer magnification of true rosettes, brisk mitotic activity, and apoptosis (C); squamous morules and inflammation (D); carcinomatous component with squamous metaplasia and atypia embedded in a myxoid spindled stroma (E). Variegated morphology with primitive, carcinomatous and sarcomatoid components (E) and lacy osteoid deposition (F). Diffuse immunoreactivity of primitive cells with anti-synaptophysin (G), anti-SALL4 nuclear reactivity (H), and SATB2 immunoreactivity within tumor (I).

4c. Case 29. Sinonasal adenocarcinoma, oncocyctic type. A-D (hematoxylin and eosin; 2x, 4x, 10x). Low power overview displaying a submucosal adenocarcinoma with back-to-back glands filling the stroma. Sinonasal adenocarcinoma, nonsalivary, nonintestinal (sero-mucinous) type, formed by bland cuboidal back-to-back glands filling the stroma. Oncocytic and vascularized appearance of tumor (A upper-half, B, B inset) and papillary growth (A lower-half, C, C inset). D: chronic lymphocytic and plasmacytoid infiltrate/stroma associated with several areas of the tumor.

4d. Case 30. High-grade sinonasal nonintestinal adenocarcinoma with blastoma component. A-D (hematoxylin and eosin; 0.5x, 4x, 10x). Scanning magnification of a submucosal carcinoma with various patterns of growth and bone invasion (A); glandular “salivary-like” pattern with areas of necrosis (right hand side) (B) and scattered sebaceous elements (right hand lower corner) (C); trabecula and ribbons of malignant cells with interspersed rosette-like glands (D, D inset).

Figure 5. Top 10 specific differentially expressed genes. Upper panels: HGNEC (blue bars) versus SNUC (yellow bars) (A- upregulated; B- downregulated) Lower panels: HGSNC (blue bars) versus SNUC (yellow bars) (C-upregulated; D- downregulated). The neuroendocrine family genes *CHGA1* and *ASCL1* had the highest values among the HGNECs. Of interest, major histocompatibility complex (MHC) class I and II members were also downregulated, along with several other chemokine family members (including CCL28 and CCL14).

Figure 6. The highest-scoring Ingenuity Pathway Analysis networks for SNUCs (A- upregulated PRAME; B- upregulated EZH2, BRCA1; C- upregulated ETV4 and downregulated MHC II) and HGNECs (D- upregulated ASCL1; E- downregulated MHC II and interleukins).

Table 1 Clinical and pathological characteristics

ID	Site/ Epicenter	Diagnosis	pTNM	Adjuvant TX	Recurrence	Follow-up (months)	Status last contact
1	Maxillary sinus	SNUC	pT4N0M1	CXRT	DM- liver met	10	DOD
2	Nasal cavity	SNUC	pT4N0M1	CXRT	DM- lung, brain	50	DOD
3	Nasal cavity	SNUC	pT4N0M0	CXRT	Local recurrence	71	AWD
4	Maxillary sinus	SNUC	pT4N0M0	XRT	no	62	NED
5	Nasal cavity	SNUC- <i>SMARCB1</i>	pT4N2M0	CXRT	Neck recurrence	33	DOD
6	Maxillary sinus	SNUC- <i>SMARCB1</i>	pT4NxM0	CXRT	no	11	Deceased
7	Maxillary sinus	SNUC	pT4N1M0	CXRT	Local recurrence	17	DOD
8	Nasal cavity	SNUC	pT4N0M0	CXRT	no	83	Deceased (CHF)

9	Nasal cavity	SNUC	pT4N0M0	CXRT	no	38	NED
10	Maxillary sinus	SNUC	pT4NxM1	CXRT	DM-liver, abdomen	11	DOD
11	Maxillary sinus	SNUC	pT4NxM1	CXRT	DM-liver, thoracic LNs, bone	10	DOD
12	Ethmoid	SNUC	pT4N2M1	CXRT and Immunotox OX40-Ig	Intraparotid and upper cervical LN, submental	36	DOD
13	Nasal cavity	SNUC	pT4N2M0	CXRT	no	34	NED
14	Sphenoid	SNUC- <i>SMARCB1</i>	pT4N0M0	CXRT	no	43	NED
15	Nasopharynx	SNUC	rpT2N0M0	CXRT	Local recurrence	64	NED
16	Nasal cavity	SNUC	pT1N0M0	XRT (proton)	no	10	NED
17	Nasal cavity	SNUC	pT2N0M0	CXRT	no	10	NED
18	Sphenoid	SNUC	pT4N0M0	CXRT	Local recurrence	60	AWD
19	Nasal cavity	Met SNUC (liver)	pT4N0M0	CXRT	DM-liver	48	AWD
20	Nasal cavity	SNUC - <i>SMARCB1</i>	pT4N0M0	CXRT	no	30	n/a
21	Nasal cavity	SNUC - <i>SMARCB1</i>	pT3N0M0	CXRT	Local recurrence	12	DOD
22	Ethmoid	LCNEC	pT4NxM0	CXRT	Local recurrence	12	AWD
23	Nasal cavity	SmCNEC	pT4NxM1	CXRT	Leptomeningeal mets, spinal mets	12	AWD
24	Maxillary sinus	SmCNEC	pT4N0M0	CXRT	Local recurrence	24	DOD
25	Nasal cavity	LCNEC	pT1N0M0	XRT	n/a	9	n/a
26	Nasal cavity	SmCNEC	pT3N0M0	CXRT	no	60	NED

27	Maxillary sinus	NUT	pT4N0M1	CXRT	Local recurrence and spinal mets	18	DOD
28	Maxillary sinus	TCS	pT4NxM0	CXRT	no	12	NED
29	Maxillary sinus	SNAC	pT2N0M0	XRT	no	12	NED
30	Maxillary sinus	SNAC "blastema"	pT4N0M0	XRT	no	10	NED

TX- treatment; SNUC- sinonasal undifferentiated carcinoma; CXRT- chemotherapy plus radiation therapy; DM- distant metastasis]; LN- lymph nodes; DOD: died of disease; AWD: alive with disease; NED: No evidence of disease; LCNEC- large cell neuroendocrine carcinoma; Sm CNEC- small cell neuroendocrine carcinoma; NUT- nuclear protein of testis carcinoma; TCS- teratocarcinoma; SNAC- sinonasal adenocarcinoma.

Highlights

1. The aim of this exploratory study was to characterize the immune-oncology gene expression profile in SNUC and other high-grade sinonasal carcinomas.
2. The immune-oncology gene expression analysis identified a number of differentially expressed transcripts reflecting effects on tumorigenesis.
3. To our knowledge, this is the first description of PRAME (preferentially expressed antigen in melanoma) with preferential expression in SNUCs, opening the avenue for further investigations as a biomarker (on larger annotated multi-institutional cohorts), and functional studies addressing immunogenicity and safety of PRAME immunotherapeutics.